

Fluctuation Induced Homochirality

Takeshi SUGIMORI*, Hiroyuki HYUGA†, and Yukio SAITO‡

Department of Physics, Keio University, Yokohama 223-8522

(Received October 31, 2018)

We propose a new mechanism for the achievement of homochirality in life without any autocatalytic production process. Our model consists of a spontaneous production together with a recycling cross inhibition in a closed system. It is shown that although the rate equations for this system predict no chiral symmetry breaking, the stochastic master equation predicts complete homochirality. This is because the fluctuation induced by the discreteness of population numbers of participating molecules plays essential roles. This fluctuation conspires with the recycling cross inhibition to realize the homochirality.

KEYWORDS: homochirality, probability distribution, master equation, recycling cross inhibition, directed random walk

1. Introduction and Model System

It has long been known since the discovery of Pasteur that organic molecules in life are homochiral, in other words, having a completely broken chiral symmetry.^{1,2} The origin of this homochirality remains an unsolved important puzzle.^{3–6} Various mechanisms for the germination of chirality imbalance have been proposed such as different intensities of circularly polarized light in a primordial era, adsorption on optically active crystals, or the parity breaking in the weak interaction.⁷

Predicted asymmetries, however, have turned out to be very small,^{5,7,8} and therefore their amplification is indispensable. Frank showed theoretically that an autocatalytic reaction accompanying cross inhibition can lead to the amplification of enantiomeric excess (ee) and to the eventual homochirality in an open system.⁹ Following this work, numerous studies have been performed on the chiral amplification and selection in various systems.^{4–6,10,11}

Recently, the amplification of ee (but not homochirality) was realized in experiments carried out by Soai et al.,^{12,13} and the temporal evolution of the chemical reaction was shown to be explained by a second-order autocatalytic reaction.^{14,15} Stimulated by these works, we proposed that, in addition to the nonlinear autocatalytic reaction, a recycling process induced by a back reaction gives rise to the complete homochirality in a closed system.¹⁶ Subsequently several theoretical works related to this mechanism have been done.^{17–22}

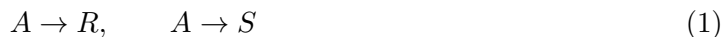
*tsugimor@rk.phys.keio.ac.jp

†hyuga@rk.phys.keio.ac.jp

‡yukio@rk.phys.keio.ac.jp

In these studies of chiral amplification, the autocatalytic reaction plays an essential role either in open systems or in closed systems.^{4–6,9–11,16–22} So far, however, any autocatalytic reaction has not been found in the process of polymerization, relevant for the formation of organic molecules in life. Granting that some pertinent autocatalytic reaction may well be discovered in future, it seems worthwhile to explore possibilities of chirality selection in non-autocatalytic way. In this paper, we demonstrate that complete chirality selection or homochirality is possible in a closed system with spontaneous production together with recycling cross inhibition but without autocatalytic reaction.

Our model consists of achiral substrate molecule A and two chiral enantiomers R and S , which are produced by spontaneous productions



with the same reaction rate k_0 . Furthermore, R and S are assumed to react back to A as



with a reaction rate μ_0 . We call this reaction a recycling cross inhibition, which looks similar to Frank's cross inhibition but differs in that whether R and S are recycled back in the present model or eliminated out of the system in the Frank's open model.⁹

In §2, the rate equation approach shows that the system has a line of fixed points and chirality selection is impossible. Since the fixed line is neutral in stability, the system is expected to be susceptible to the weakest perturbations such as fluctuation. The rate equation, however, describes only the evolution of average quantities. To include fluctuation effect, one has to consider stochastic aspects of the system evolution. This feature can be taken into account in a stochastic master equation approach, where the system is described by a probability distribution function.^{23–25} From stochastic analysis in §3 and §4, it will be shown that the fluctuation drives the system to homochirality. The effect of the fluctuation is attributed to the discreteness of the microscopic process, the essence of which is extracted in the system size expansion in §5. The result is summarized in §6.

2. Rate equation approach

In the rate equation approach, the reaction processes, Eq.(1) and Eq.(2), are expressed as

$$\frac{dr}{dt} = k_0 a - \mu_0 r s, \quad (3)$$

$$\frac{ds}{dt} = k_0 a - \mu_0 r s, \quad (4)$$

together with

$$c = a + r + s \quad (5)$$

where a, r, s are concentrations of species A, R, S respectively and the total concentration c is assumed to be constant. The conservation of total concentration expressed by Eq.(5) implies that R and S are recycled back to A via the cross inhibition reaction ($-\mu_0 rs$). The trajectories of the evolution are easily obtained as $r - s = \text{constant}$, as shown by lines with arrows in Fig. 1. The final states are obtained by solving $\dot{r} = \dot{s} = k_0 a - \mu_0 rs = 0$ together with $a + r + s = c$, resulting the following hyperbola

$$\left(\frac{r}{c} + \frac{k_0}{c\mu_0}\right)\left(\frac{s}{c} + \frac{k_0}{c\mu_0}\right) = \frac{k_0}{c\mu_0}\left(1 + \frac{k_0}{c\mu_0}\right) \quad (6)$$

as is shown in Fig. 1. There, the rate for the cross inhibition μ_0 is chosen to be very large compared to that for the spontaneous production k_0 as $c\mu_0 = 5k_0$, in order to draw the fixed line of hyperbola clearly visible away from the diagonal boundary line $r + s = c$. We expect, however, that the cross inhibition, if it exists, should be a very rare process and $c\mu_0 \ll k_0$. The conclusion of this rate equation approach is that the enantiomeric excess (ee) defined as

$$\phi = \frac{r - s}{r + s} \quad (7)$$

takes any value ($-1 \leq \phi \leq 1$), depending on initial conditions, thus indicating no chirality selection.

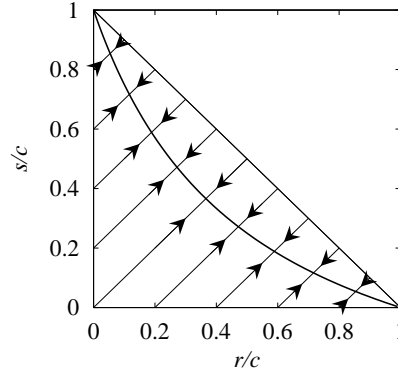


Fig. 1. Trajectory of the concentration r and s , prescribed by the rate equations (3) and (4), with a fixed line of hyperbola. The parameter is set as $c\mu_0 = 5k_0$.

There is, however, a subtle feature such that, along the fixed line (hyperbola), the system is neither stable nor unstable, namely it is neutral. Fluctuations could be decisive to destruct this neutrality and resolve the hyperbola into a few fixed points. In fact, a similar situation with a neutral fixed line appears for a closed system with a nonlinear autocatalytic process. We have adopted a stochastic master equation approach for this system, and found chiral symmetry breaking in a previous paper.²⁵ Therefore, we adopt the same approach for the present system in the following sections.

3. Master equation approach

For the stochastic approach, the relevant system is to be described in a microscopic way. Namely, the system is confined in a fixed volume V , containing species A, R, S with population numbers N_A, N_R, N_S , respectively. Total population number of all molecules is assumed to be constant $N = cV$ since the system is closed, so that we have

$$N = N_A + N_R + N_S. \quad (8)$$

Chemical reaction is assumed to be stochastic where a microscopic state specified by the population number $\mathbf{X} = (N_A, N_R, N_S)$ varies according to a certain transition probabilities $W(\mathbf{X}; \mathbf{q})$ of a jump $\mathbf{q} = (q_A, q_R, q_S)$ to another state $\mathbf{X}' = \mathbf{X} + \mathbf{q}$. The probability $P(\mathbf{X}, t)$ of a state \mathbf{X} at time t then evolves according to the master equation

$$\frac{\partial P(\mathbf{X}, t)}{\partial t} = \sum_{\mathbf{q}} W(\mathbf{X} - \mathbf{q}; \mathbf{q}) P(\mathbf{X} - \mathbf{q}, t) - \sum_{\mathbf{q}} W(\mathbf{X}; \mathbf{q}) P(\mathbf{X}, t). \quad (9)$$

The summation by \mathbf{q} is restricted by the conservation condition Eq.(8). The transition probabilities for the present model is explicitly expressed as

$$\begin{aligned} W(N_A, N_R, N_S; -1, +1, 0) &= k_0 N_A, \\ W(N_A, N_R, N_S; -1, 0, +1) &= k_0 N_A, \\ W(N_A, N_R, N_S; +2, -1, -1) &= \mu N_R N_S \end{aligned} \quad (10)$$

and those with other \mathbf{q} 's vanish. As is confirmed later, the coefficient for the microscopic cross inhibition μ is related to the macroscopic reaction rate μ_0 as

$$\mu = \frac{\mu_0}{V} = \frac{c\mu_0}{N}. \quad (11)$$

Thus the master equation in concrete form is expressed as

$$\begin{aligned} \frac{\partial P(N_A, N_R, N_S, t)}{\partial t} &= k_0(N_A + 1) \left\{ P(N_A + 1, N_R - 1, N_S, t) + P(N_A + 1, N_R, N_S - 1, t) \right\} \\ &\quad + \mu(N_R + 1)(N_S + 1) P(N_A - 2, N_R + 1, N_S + 1, t) \\ &\quad - \{2k_0 N_A + \mu N_R N_S\} P(N_A, N_R, N_S, t). \end{aligned} \quad (12)$$

Because of the conservation condition Eq.(8) the microscopic state of the system is specified by two independent variables N_R and N_S in a triangular region

$$0 \leq N_R, N_S, N_R + N_S \leq N, \quad (13)$$

as shown in Fig. 2. Transition probabilities W connect neighboring states linked along square edges or along a diagonal, indicated in Fig. 2. The system is equivalent to the directed random walk model where a random walker jumps to the right (+1 in N_R direction), to upwards (+1 in N_S direction) and to the left-down diagonal (-1 in both N_R and N_S directions) in the $N_R - N_S$ phase space. One then notices easily that two homochiral states $(N_R, N_S) = (N, 0)$ and $(0, N)$ are special; there is only inflow but no outflow of the walker, namely the transition

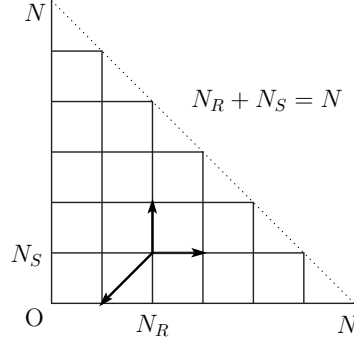


Fig. 2. Random walk in a triangular region in $N_R - N_S$ space. A walker at a site (N_R, N_S) jumps along square edges or along a diagonal indicated by arrows.

probabilities from the microscopic homochiral states $(N_A, N_R, N_S) = (0, N, 0)$ and $(0, 0, N)$ to other states are zero,

$$W(0, N, 0; \mathbf{q}) = W(0, 0, N; \mathbf{q}) = 0 \quad (14)$$

for any jump \mathbf{q} , so that, once the system enters into this homochiral states, it remains there. In this sense, the homochiral states are regarded as a sink or a kind of black hole. All other microscopic states are connected directly or indirectly to these two homochiral states, and consequently the probabilities of the other states evolve into zero, namely $P(N_A, N_R, N_S; t = \infty) = 0$ for non-homochiral states. This can be demonstrated step-by-step as follows. Because of Eq.(14), the master equation for the homochiral state takes the form

$$\frac{\partial P(0, N, 0, t)}{\partial t} = k_0 P(1, N - 1, 0, t). \quad (15)$$

In the asymptotic limit where every temporal evolution has died out $\partial P / \partial t = 0$, the asymptotic value for this neighboring state becomes $P(1, N - 1, 0, t = \infty) = 0$. Furthermore, asymptotic limit of the master equation for a general state \mathbf{X} becomes

$$\sum_{\mathbf{q}} W(\mathbf{X} - \mathbf{q}; \mathbf{q}) P(\mathbf{X} - \mathbf{q}, \infty) = \sum_{\mathbf{q}} W(\mathbf{X}; \mathbf{q}) P(\mathbf{X}, \infty) \quad (16)$$

so that if $P(\mathbf{X}, \infty) = 0$, then all the probabilities of states \mathbf{X}' connected directly to the state \mathbf{X} with positive W 's must have vanishing asymptotic values $P(\mathbf{X}', \infty) = 0$. Since every state is interconnected, this completes the proof.

This conclusion is confirmed numerically by solving the time development of the master equation Eq.(12) by using the Runge-Kutta method of the fourth order.²⁶ Starting from a completely achiral initial condition with $N_A = N$ and no chiral ingredients $N_R = N_S = 0$, the probability distribution, started from the initial delta-peak $P(N_A, N_R, N_S, t = 0) = \delta_{N_A, N} \delta_{N_R, 0} \delta_{N_S, 0}$, remains symmetric at any time, as shown in Fig. 3. There, the redundant variable $N_A = N - N_R - N_S$ is suppressed, and the probability distribution is shown in N_R and N_S phase space. The probability contour is also shown at the basement. In this

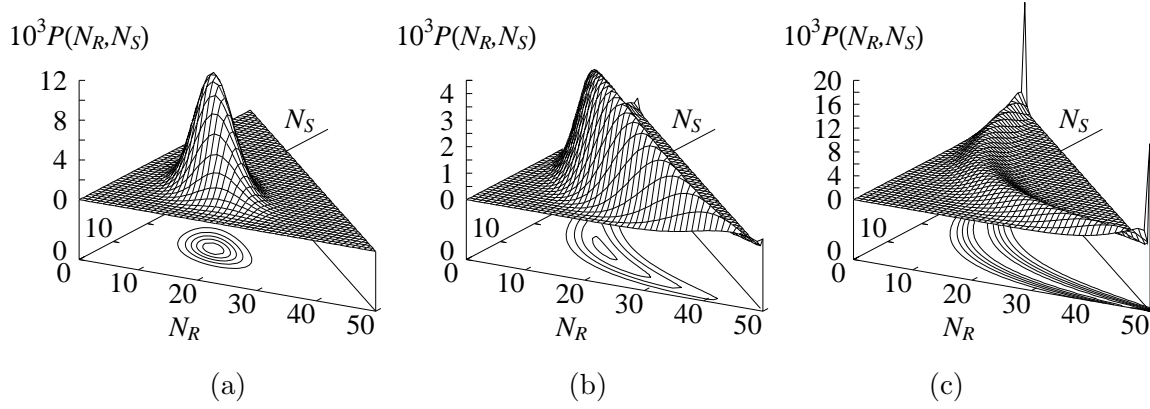


Fig. 3. Time evolution of the probability distribution with trajectory of the probability contour at the basement, obtained by numerically integrating the master equation (9) for $\mu = k_0/10$. The system starts from $P(N, 0, 0) = 1$ and depicted times are at (a) $k_0 t = 1$, (b) $k_0 t = 9$ and (c) $k_0 t = 19$. The total population number is $N = 50$.

numerical calculation, the total population number is set as $N = 50$ due to the limitation of the calculational capacity and $\mu = k_0/10$ (or $c\mu_0 = 5k_0$ as in Fig. 1) for the sake of visibility of distribution. In the early stage at a time $k_0 t = 1$ in Fig.3(a), the probability distribution has an approximately Gaussian shape with a central peak at the racemic fixed point $N_R = N_S = (k_0/\mu)(\sqrt{N\mu/k_0 + 1} - 1) \approx 14.5$ in agreement with results obtained by the rate equations. At the intermediate time $k_0 t = 9$, the probability distribution spreads along the hyperbola which is the fixed line found in the rate equation approach, as shown in Fig.3(b). In the late stage, the probability distribution develops sharp peaks at the two end points corresponding to the two homochiral states (Fig. 3(c)).

By the use of this probability distribution, an expectation value of any function $f(N_A, N_R, N_S)$ at a time t is easily calculated as

$$\langle f(N_A, N_R, N_S) \rangle_t = \sum_{N_A, N_R, N_S} f(N_A, N_R, N_S) P(N_A, N_R, N_S, t) \quad (17)$$

In Fig. 4, the time development of the expectation value of the population number of R species $\langle N_R \rangle_t$ is shown. In the early stage in Fig. 4(a), the average $\langle N_R \rangle_t$ increases sharply to the racemic fixed point value 14.5 predicted by the rate equation within a time scale of $k_0 t \approx 1$. This development is well described by the rate equations Eq.(3) and Eq.(4) together with Eq.(5), as is shown by a dashed curve in Fig. 4(a). The results by the rate equations completely agree with the evolution of average value $\langle N_R \rangle_t$ until $k_0 t \approx 1$. Then, the rate equations predict the saturations at the racemic value, but the numerical simulation of the master equations indicates a slow increase. The average $\langle N_R \rangle_t$ approaches ultimately to the value $N/2$, corresponding to the double peak profile of the final probability distribution at

the two homochiral states. The slow approach is expressed well by the following form

$$\langle N_R \rangle_t = \frac{N}{2} - Ae^{-t/\tau}. \quad (18)$$

This exponential behavior is evident in Fig. 4(b) where the logarithmic difference $\ln[N/2 - \langle N_R \rangle_t]$ is plotted versus $k_0 t$. The fitting gives values $A = 10$ and $1/k_0 \tau = 0.0163$.

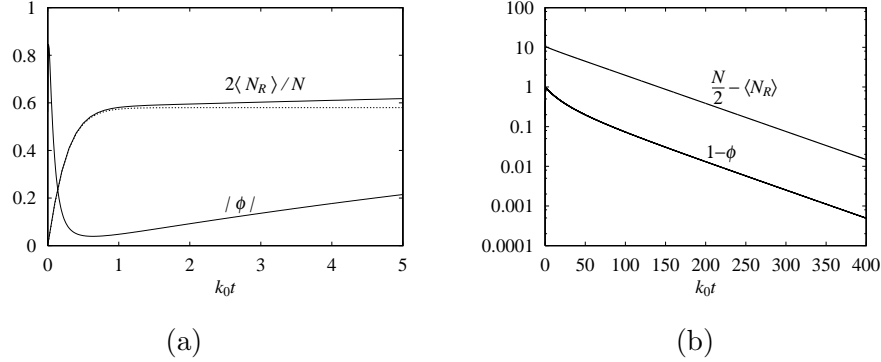


Fig. 4. Time development of the average population $\langle N_R \rangle_t$ and the absolute value of the ee order parameter $|\phi|$. (a) In an early stage, $k_0 t \leq 1$, $\langle N_R \rangle_t$ agrees with the evolution by the rate equation, which is shown by a dashed curve. (b) Exponential relaxation in the asymptotic region.

The enantiomeric excess (ee) corresponds to an order parameter in a phase transition in standard statistical mechanics. Adopting an analogous definition of an order parameter in numerical simulations for magnetic phase transitions, we define the absolute value of ee as

$$|\phi(t)| = \left\langle \left(\frac{N_R - N_S}{N_R + N_S} \right)^2 \right\rangle_t^{1/2}. \quad (19)$$

The time development of an ee order parameter $|\phi|$ is also shown in Fig. 4(a) and (b). In the very early stage $k_0 t \leq 0.2$ in Fig. 4(a) $|\phi|$ is very large because the probability has a large amplitude close to the edges $N_R = 0$ or $N_S = 0$. As time evolves, the numbers of R and S molecules increase and the peak position of the probability distribution leaves from both edges (Fig. 3(a)), and thus the ee value $|\phi|$ drops sharply. After the peak of the probability distribution reaches the racemic fixed point where $|\phi| \approx 0$, the probability spreads along the fixed line (Fig. 3(b)), and thus $|\phi|$ value increases steadily to a final value, unity, of homochirality. By plotting the logarithm of the difference, $\ln[1 - |\phi(t)|]$, as a function of $k_0 t$, as in Fig. 4(b), one again obtains the exponential relaxation with the same exponent $1/k_0 \tau \approx 0.0162$.

4. Eigenvalue Analysis

The asymptotic relaxation of the average value and the ee order parameter turned out to be exponential with the same characteristic time, $k_0 \tau \approx 60$. We consider this problem in terms of eigenvalues of evolution matrix of the master equation. Since master equation is a linear

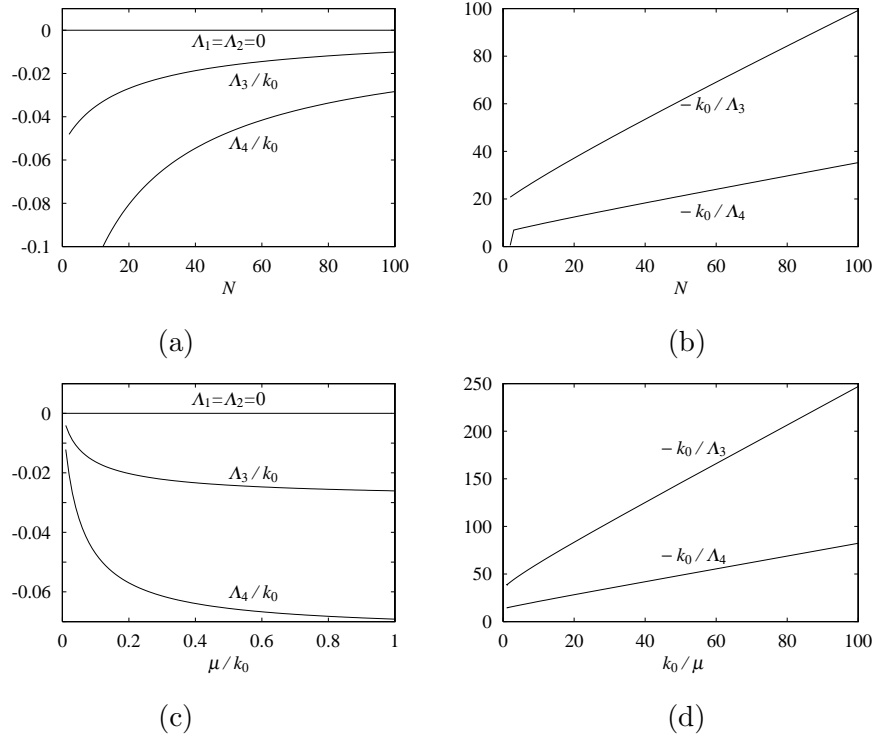


Fig. 5. A few largest eigenvalues Λ_i of the time-evolution matrix plotted (a) versus total population N at a fixed cross inhibition, $\mu/k_0 = 0.1$, and (c) versus μ/k_0 at a fixed $N = 50$. By plotting the inverse of eigenvalues in (b) and (d), one finds $k_0/|\Lambda_i|$ is linear in N and also in k_0/μ , asymptotically.

equation for the probability distribution, the time evolution is written by using the evolution matrix \mathbf{M}

$$\frac{dP(\mathbf{X}, t)}{dt} = \sum_{\mathbf{X}'} (\mathbf{X}|\mathbf{M}|\mathbf{X}') P(\mathbf{X}', t), \quad (20)$$

where matrix elements of \mathbf{M} are related to the transition probabilities W as

$$(\mathbf{X}|\mathbf{M}|\mathbf{X}') = \begin{cases} W(\mathbf{X}'; \mathbf{X} - \mathbf{X}') & \text{for } \mathbf{X}' \neq \mathbf{X}, \\ -\sum_{\mathbf{q}} W(\mathbf{X}; \mathbf{q}) & \text{for } \mathbf{X}' = \mathbf{X}. \end{cases} \quad (21)$$

By the use of eigenfunctions Ψ_i and eigenvalues Λ_i of the matrix \mathbf{M} as

$$\mathbf{M}\Psi_i = \Lambda_i\Psi_i, \quad (22)$$

the time development of the probability distribution is expressed as a series

$$P(\mathbf{X}, t) = \sum_{i=1}^{\infty} a_i e^{\Lambda_i t} \Psi_i. \quad (23)$$

Since the probability distribution satisfies the conservation as $\sum_{\mathbf{X}} P(\mathbf{X}, t) = 1$, all the eigenvalues must be non-positive. In the previous section, we have proven that two homochiral states corresponds to the final states, so that there are two degenerate zero eigenvalues $\Lambda_1 = \Lambda_2 = 0$

with eigenstates $\Psi_1 = \delta_{N_A,0}\delta_{N_R,N}\delta_{N_S,0}$ and $\Psi_2 = \delta_{N_A,0}\delta_{N_R,0}\delta_{N_S,N}$, or their linear combinations. The asymptotic temporal evolution is governed then by the third largest eigenvalue Λ_3 .

One can calculate eigenvalues of the matrix \mathbf{M} numerically by using the subroutine "dgeev" in LAPACK. A few largest eigenvalues are shown in Fig. 5 as a function of the total population number N for a fixed cross inhibition $\mu = 0.1k_0$ (Figs. 5(a) and (b)), or as a function of μ/k_0 for a fixed $N = 50$ (Figs. 5(c) and (d)). For $\mu = 0.1k_0$ and $N = 50$, the third largest eigenvalue has a value $\Lambda_3/k_0 = -0.0163$, in good agreement with the exponent $1/k_0\tau = 0.0163$ obtained in the previous section from the asymptotic final relaxation of the average $\langle N_R \rangle_t$ and the ee values $|\phi(t)|$.

By plotting the inverse of eigenvalues $-k_0/\Lambda_i$ as in Figs. 5(b) and (d), one notices that it is linear in the total population number N and the inverse strength of the cross inhibition k_0/μ , asymptotically. Therefore, for a very large system with a small cross inhibition, it should take a long time of the order N/μ before the homochirality becomes observable.

5. System size expansion

For our model with spontaneous production of chiral species with recycling cross inhibition, the rate equation tells us no chirality selection whereas the stochastic master equation insists the final configuration be homochiral. The totally different conclusions are ascribed to the fluctuation due to the discreteness of microscopic processes. The fluctuation effect associated to the system size is qualitatively analyzed by the system size (precisely said, the inverse system size) expansion analysis of the master equation, developed by R. Kubo et al.^{27,28}

In the master Eq.(9), the probability density $P(\mathbf{X}, t)$ of a microscopic state \mathbf{X} is connected to another state $\mathbf{X} + \mathbf{q}$ which differs with a jump \mathbf{q} of order unity by a transition probability $W(\mathbf{X}; \mathbf{q})$. The rate W is of macroscopic order of the system size N or the volume V as

$$W(\mathbf{X}; \mathbf{q}) = Vw(\mathbf{x}; \mathbf{q}) \quad (24)$$

where \mathbf{x} is the density variable $\mathbf{x} = \mathbf{X}/V$ of order unity:

$$\mathbf{x} = (a, r, s) = \left(\frac{N_A}{V}, \frac{N_R}{V}, \frac{N_S}{V} \right). \quad (25)$$

Then, the probability is assumed to take the form $P(\mathbf{X}, t) = \exp[V\chi(\mathbf{x}, t)]$, and time evolutions of the leading order contributions of the average density $\langle \mathbf{x} \rangle_t$ and the correlation functions

$$\sigma_{ij}(t) = V \langle (x_i - \langle x_i \rangle_t)(x_j - \langle x_j \rangle_t) \rangle \quad (26)$$

are shown to be determined by moments

$$c_{ij\dots}(\mathbf{x}) = \sum_{\mathbf{q}} q_i q_j \dots w(\mathbf{x}; \mathbf{q}) \quad (27)$$

of the transition probability w as

$$\begin{aligned}\frac{d}{dt}\langle x_i \rangle_t &= c_i(\langle \mathbf{x} \rangle_t) \\ \frac{d}{dt}\sigma_{ij}(t) &= \sum_k \left(\frac{\partial c_i}{\partial \langle x_k \rangle_t} \sigma_{kj}(t) + \sigma_{ik}(t) \frac{\partial c_j}{\partial \langle x_k \rangle_t} \right) + c_{ij}(\langle \mathbf{x} \rangle_t).\end{aligned}\quad (28)$$

The evolution equations for the higher order corrections can also be derived.²⁷ If the system is normal, the fluctuation correlations σ_{ij} remains of order unity. On the other hand, if the system is unstable, as in the case of phase transitions with critical behaviors, at least one of the fluctuations σ_{ij} is enhanced to the order of the system size.

In the present model, first order moments are

$$c_r = c_s = k_0 a - \mu_0 r s = k_0(c - r - s) - \mu_0 r s \quad (29)$$

and the second order moments are

$$c_{rr} = c_{ss} = k_0 a + \mu_0 r s = k_0(c - r - s) + \mu_0 r s, \quad c_{rs} = \mu_0 r s, \quad (30)$$

where $\mu_0 = V\mu$ as defined previously in Eq.(11). Thus, the lowest order of the average concentrations $\langle r \rangle_t$ and $\langle s \rangle_t$ satisfy the rate equations Eq.(3) and Eq.(4). For simplicity, we describe these lowest order average values as r and s , hereafter. The correlation functions follow the evolution

$$\begin{aligned}\frac{d}{dt}\sigma_{rr}(t) &= -2(k_0 + \mu_0 s)\sigma_{rr} - 2(k_0 + \mu_0 r)\sigma_{rs} + k_0(c - r - s) + \mu_0 r s \\ \frac{d}{dt}\sigma_{rs}(t) &= -(k_0 + \mu_0 s)\sigma_{rr} - (2k_0 + \mu_0 r + \mu_0 s)\sigma_{rs} - (k_0 + \mu_0 r)\sigma_{ss} + \mu_0 r s \\ \frac{d}{dt}\sigma_{ss}(t) &= -2(k_0 + \mu_0 r)\sigma_{ss} - 2(k_0 + \mu_0 s)\sigma_{rs} + k_0(c - r - s) + \mu_0 r s\end{aligned}\quad (31)$$

To detect the chiral symmetry breaking, it is more convenient to use the following symmetric and asymmetric variables

$$x_+ = r + s, \quad x_- = r - s. \quad (32)$$

Their averages and correlation functions evolve as

$$\begin{aligned}\frac{d}{dt}x_+ &= 2k_0(c - x_+) - \frac{1}{2}\mu_0(x_+^2 - x_-^2), \quad \frac{d}{dt}x_- = 0, \\ \frac{d}{dt}\sigma_{++} &= -2(2k_0 + \mu_0 x_+)\sigma_{++} + 2k_0(c - x_+) + \mu_0(x_+^2 - x_-^2), \\ \frac{d}{dt}\sigma_{+-} &= -(2k_0 + \mu_0 x_+)\sigma_{+-} + \mu_0 x_- \sigma_{--}, \quad \frac{d}{dt}\sigma_{--} = 2k_0(c - x_+).\end{aligned}\quad (33)$$

By starting from the completely achiral initial condition, the system remains racemic with average value $x_- = 0$, and x_+ approaches to the racemic fixed point value $(2k_0/\mu_0)(\sqrt{c\mu_0/k_0 + 1} - 1)$. The time the system takes to reach the racemic fixed point is of order $1/k_0$.

The fluctuation of the asymmetry variable σ_{--} , however, increases indefinitely in this approximation. In fact, when the average value of x_+ takes the racemic point value, the fluctuation increases linearly in time with a positive velocity;

$$\frac{\dot{\sigma}_{--}}{c} = \frac{1}{2} \frac{\mu_0}{c} x_+^2 = \frac{1}{2} N \mu \left(\frac{x_+}{c} \right)^2 > 0. \quad (34)$$

This increase of the fluctuation indicates that the discreteness in the microscopic process of chemical reaction evokes an intrinsic instability of the racemic fixed point (and in general, every points on the fixed line) to macroscopic level.

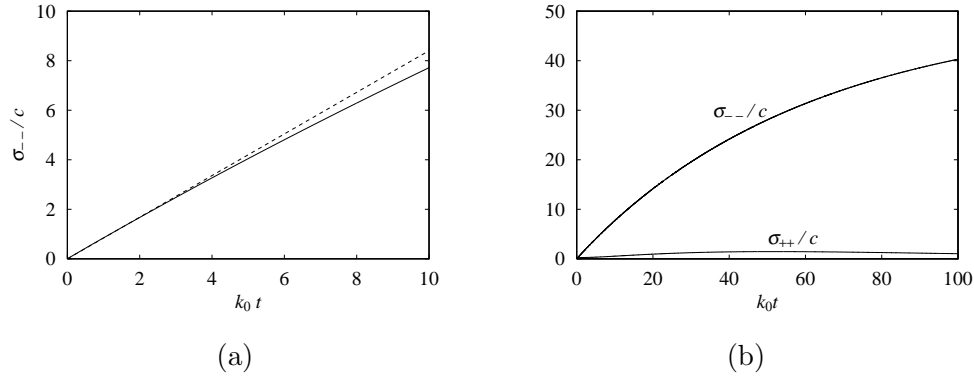


Fig. 6. Fluctuation correlation functions obtained by numerically time integrating the master equation (a) at an early stage, and (b) a whole time range. Parameter is set as $\mu = k_0/10$, or $c\mu_0 = 5k_0$. A dotted line in (a) represents the result of system size expansion.

In the numerical simulation the fluctuation of asymmetric variable $\sigma_{--}(t)/c$ actually increases in time, as shown in Fig. 6. The initial increase shown by a continuous curve in Fig. 6(a) is linear in time $k_0 t$, as expected from the system size expansion analysis, shown by a dashed line. As time passes, the system size analysis fails, since the average value x_+ deviates from the racemic value in the actual simulation. One then has to consider higher order contributions to the average of x_+ . Departure from the racemic state becomes visible in a macroscopic sense when the fluctuation expressed by σ_{--}/c reaches the order N . The time for this to appear is of order $1/\mu$, as is obtained from Eq.(34) and by assuming $x_+ \sim c$.

Asymptotically, the double peak structure develops in the probability distribution. The time scale for this to fully develop is governed by the largest nonzero eigenvalue Λ_3 so that the homochirality is realized in the time of order of $1/|\Lambda_3| \approx N/\mu$, as is described in the previous section.

6. Conclusion and discussion

It seems to be a general consensus that an autocatalytic production process, either linear or nonlinear, is indispensable for the realization of homochirality. In the present work, we

proposed a new mechanism by using a simple model to demonstrated that the homochirality can be realized without any autocatalytic production process. Our model consists of a spontaneous production together with a recycling cross inhibition in a closed system. As was shown, the rate equations for this system predict no chiral symmetry breaking, but the stochastic master equation predicts complete homochirality. This is because the fluctuation induced by the discreteness of population numbers of participating molecules plays essential roles. This fluctuation conspires with the recycling cross inhibition to realize the homochirality.

If this fluctuation mechanism could explain the homochirality in life, then this is what Pearson suggested long time ago.²⁹ However, the necessary time for the homochirality to set in due to the fluctuation is very large, as it is proportional to the total number of the relevant molecules ($\approx N/\mu$), which is of macroscopic size. Taking this feature into account, we can conceive a new senario for the homochirality in macroscopic scale as follows. At first, in some small closed corner, such as in a region enclosed by a vesicle, the fluctuation induced homochirality is realized in a very long time with respect to the time scale of laboratory experiments, but not so long with respect to geological time scale. It may be conceivable that in this period some unknown autocatalytic reaction, the effect of which is too small to be detected in the laboratory experiment so far, begins to operate and generates the large scale realization of the homochiralty from the homochiral seeds produced by the fluctuation mechanism proposed here.

Even though reaction systems with a recycling cross inhibition are not yet found, we hope that a simple system with only a recycling cross inhibition might be found in near future, and the establishment of homochirality be checked.

Acknowledgement

Y. S. acknowledges support by a Grant-in-Aid for Scientific Research (No. 19540410) from the Japan Society for the Promotion of Science.

References

- 1) L. Pasteur: *Comptes Rendus*, **26** (1848) 535.
- 2) F. R. Japp: *Nature* **58** (1898) 452.
- 3) L. Stryer: *Biochemistry* (Feeman and Comp., New York, 1998).
- 4) M. Calvin: *Chemical Evolution* (Oxford University Press, Oxford, 1969).
- 5) V. I. Goldanskii and V. V. Kuz'min: *Z. Phys. Chem. (Leipzig)* **269** (1988) 216.
- 6) I. D. Gridnev: *Chem. Lett.* **35** (2006) 148.
- 7) See for example a review by B. L. Feringa and R. A. van Delden: *Angew. Chem. Int. Ed.* **38** (1999) 3419.
- 8) M. H. Mills: *Chem. Ind. (London)* **51** (1932) 750.
- 9) F. C. Frank: *Biochimi. Biophys. Acta* **11** (1953) 459.
- 10) P. G. H. Sandars: *Orig. Life. Evol. Biosph.* **33** (2003) 575.
- 11) A. Brandenburg and T. Multamaki: *Int. J. Astrobiol.* **3** (2004) 209.
- 12) K. Soai, T. Shibata, H. Morioka, and K. Choji: *Nature* **378** (1995) 767.
- 13) K. Soai, T. Shibata, and I. Sato: *Acc. Chem. Res.* **33** (2000) 382.
- 14) I. Sato, D. Omiya, K. Tsukiyama, Y. Ogi, and K. Soai: *Tetrahedron: Asymmetry* **12** (2001) 1965.
- 15) I. Sato, D. Omiya, H. Igarashi, K. Kato, Y. Ogi, K. Tsukiyama, and K. Soai: *Tetrahedron: Asymmetry* **14** (2003) 975.
- 16) Y. Saito, and H. Hyuga: *J. Phys. Soc. Jpn.* **73** (2004) 33.
- 17) Y. Saito, and H. Hyuga: *J. Phys. Soc. Jpn.* **73** (2004) 1685.
- 18) Y. Saito, and H. Hyuga: *J. Phys. Soc. Jpn.* **74** (2005) 535.
- 19) Y. Saito, and H. Hyuga: *J. Phys. Soc. Jpn.* **74** (2005) 1629.
- 20) Y. Saito, and H. Hyuga: in *Progress in Chemical Physics Research*, ed. A. N. Linke, Ch.3, (NOVA, New York, 2005) p.65.
- 21) R. Shibata, Y. Saito, and H. Hyuga: *Phy. Rev. E* **74** (2006) 026117.
- 22) Y. Saito and H. Hyuga: in *Topics in Current Chemistry: Amplification of Chirality*, ed. K. Soai, (Springer, Heidelberg, 2007).
- 23) G. Lente: *J. Phys. Chem.* **108** (2004) 9475.
- 24) G. Lente: *J. Phys. Chem.* **109** (2005) 11058.
- 25) Y. Saito, T. Sugimori and H. Hyuga: *J. Phys. Soc. Jpn.* **76** (2007) 044802.
- 26) W. H. Press, S. A. Teukolsky, W. T. Vetterling and B. P. Flannery, *Numerical Recipes in Fortran* (Cambridge University Press, Cambridge, 1992).
- 27) R. Kubo, K. Matsuo and K. Kitahara; *J. Stat. Phys.* **9** (1973) 51.
- 28) Y. Saito and R. Kubo; *J. Stat. Phys.* **15** (1976) 233.
- 29) K. Pearson: *Nature* **58** (1898) 496, *ibid* **59** (1898) 30.